A Gaussian Beam Forward Model for Quantitative Optical Coherence Tomography

RICAM Special Semester WS2, Linz, Oktober 17.-21., 2022

joint work with:

Lisa Krainz[1], Leonidas Mindrinos[3], Wolfgang Drexler[1] and Peter Elbau[2]

[1] Medical University of Vienna
[2] University of Vienna, Faculty of Mathematics
[3] Agricultural University of Athens

Leopold Veselka

Der Wissenschaftsfonds.

Optical coherence tomography (OCT):

- produces high-resolution images
- main field of application: ophthalmology and human skin imaging
  $\rightarrow$ instrument in medical diagnosis

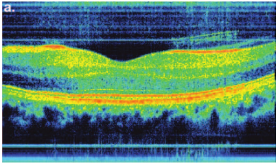

D. Huang, E. A. Swanson, C. P. Lin, J. S. Schuman, G. Stinson, W. Chang, M. R. Hee, T. Flotte, K. Gregory, C. A. Puliafito, and J. G. Fujimoto (1991). "Optical coherence tomography". In: *Science* 254.5035, pp. 1178–1181. ISSN: 0036-8075

W. Drexler and J. G. Fujimoto (2015). *Optical Coherence Tomography: Technology and Applications*. 2nd ed. Switzerland: Springer International Publishing

A. F. Fercher (1996). "Optical coherence tomography". In: *Journal of Biomedical Optics* 1.2, pp. 157–173. ISSN: 1083-3668

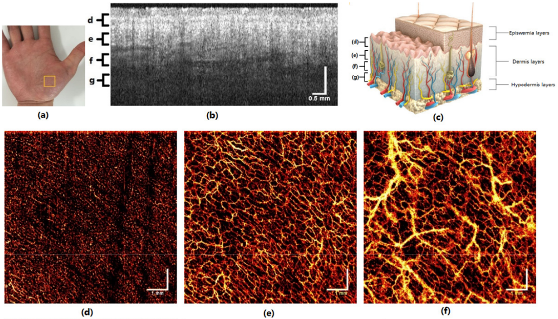

Figure: OCT angiographic tomogram of the human palm.
(d)-(f) en-face view of axial projection of given depth.

W. Drexler and J. G. Fujimoto (2015). *Optical Coherence Tomography: Technology and Applications*. 2nd ed. Switzerland: Springer International Publishing

Z. Chen, M. Liu, M. Minneman, L. Ginner, E. Hoover, H. Sattmann, M. Bonesi, W. Drexler, and R. A. Leitgeb (2016). "Phase-stable swept source OCT angiography in human skin using an akinetic source". In: *Biomedical Optics Express* 7.8, pp. 3032–3048. DOI: 10.1364/boe.7.003032

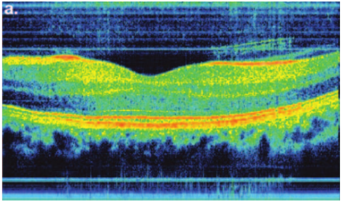

Figure: Human makula obtained a Fourier domain OCT system.

Optical coherence tomography (OCT):

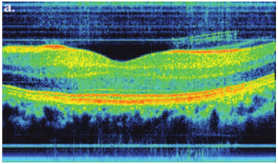

- produces high-resolution images
- main field of application: ophthalmology and human skin imaging
  $\rightarrow$ instrument in medical diagnosis

Major drawback: OCT images only provide qualitative information.

Quantitative OCT

The quantification of material information (i.e. optical or mechanical) from (interference) data obtained by an optical coherence tomographic system.

D. Huang, E. A. Swanson, C. P. Lin, J. S. Schuman, G. Stinson, W. Chang, M. R. Hee, T. Flotte, K. Gregory, C. A. Puliafito, and J. G. Fujimoto (1991). "Optical coherence tomography". In: *Science* 254.5035, pp. 1178–1181. ISSN: 0036-8075

A. F. Fercher (1996). "Optical coherence tomography". In: *Journal of Biomedical Optics* 1.2, pp. 157–173. ISSN: 1083-3668

W. Drexler and J. G. Fujimoto (2015). *Optical Coherence Tomography: Technology and Applications*. 2nd ed. Switzerland: Springer International Publishing

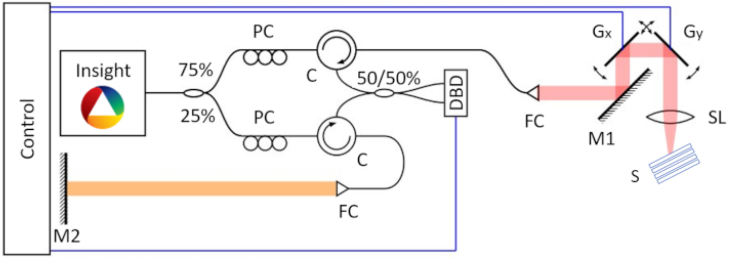
Control
Insight
75%
25%
PC
PC
C
C
50/50%
DBD
FC
FC
M2
Gx
Gy
M1
SL
S

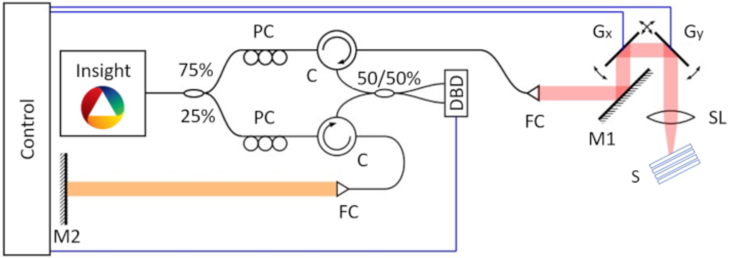

Measurement in SS-OCT: let $E_S, E_R : \mathbb{R} \times \mathbb{R}^3 \to \mathbb{C}^3$ denote the sample and the reference field respectively

$$(I)\ \left|E_S + E_R\right|^2 \quad (II)\ \left|E_S\right|^2 \quad (III)\ \left|E_R\right|^2, \quad \text{for } (k, x) \in \mathcal{S} \times \mathcal{D} \subset \mathbb{R} \times \mathbb{R}^3$$

Cross-correlation:

$$C(k, x) = (I) - (II) - (III) = 2\,\Re\mathrm{e}\left\{E_S(k, x) \cdot \overline{E_R(k, x)}\right\}$$

Quantitative Reconstruction in OCT

Assume the object is located inside a bounded domain $\Omega \subset \mathbb{R}^3$ and is characterized by the refractive index

$$n : \mathbb{R} \times \mathbb{R}^3 \to \mathbb{C},\ (k, x) \mapsto n(k, x),$$

with $n = 1$ outside Ω and $k = 2\pi/\lambda$ denotes the wavenumber.

universität wien

Quantitative Reconstruction in OCT

Assume the object is located inside a bounded domain $\Omega \subset \mathbb{R}^3$ and is characterized by the refractive index

$$n : \mathbb{R} \times \mathbb{R}^3 \to \mathbb{C},\ (k, x) \mapsto n(k, x),$$

with $n = 1$ outside Ω and $k = 2\pi/\lambda$ denotes the wavenumber.

Given the measurement data obtained by an OCT system, we are interested in extracting the refractive index of the underlying object from this data.

This means we are interested in inverting the equation

$$F(n) = C$$

where F represents the OCT forward model.

Works on Quantitative Reconstruction in OCT

A. F. Fercher, C. K. Hitzenberger, G. Kamp, and S. Y. El Zaiat (1995). “Measurement of intraocular distances by backscattering spectral interferometry”. In: *Optics Communications* 117, pp. 43–48

A. F. Fercher (1996). “Optical coherence tomography”. In: *Journal of Biomedical Optics* 1.2, pp. 157–173. ISSN: 1083-3668

T. S. Ralston, D. L. Marks, P. S. Carney, and S. A. Boppart (2006). “Inverse scattering for optical coherence tomography”. In: *Journal of the Optical Society of America A* 23.5, pp. 1027–1037. ISSN: 0764-583X

D. L. Marks, T. S. Ralston, S. A. Boppart, and P. S. Carney (2007). “Inverse scattering for frequency-scanned full-field optical coherence tomography”. In: *Journal of the Optical Society of America A* 24.4, pp. 1034–1041. ISSN: 0764-583X

O. Bruno and J. Chaubell (2005). “One-dimensional inverse scattering problem for optical coherence tomography”. In: *Inverse Problems* 21, pp. 499–524. ISSN: 0266-5611

P. H. Tomlins and R. K. Wang (2005). “Theory, developments and applications of optical coherence tomography”. In: *Journal of Physics D: Applied Physics* 38, pp. 2519–2535

P. Elbau, L. Mindrinos, and O. Scherzer (2015). “Mathematical Methods of Optical Coherence Tomography”. In: *Handbook of Mathematical Methods in Imaging*. Ed. by O. Scherzer. Springer New York, pp. 1169–1204. DOI: `10.1007/978-1-4939-0790-8_44`. URL: `http://link.springer.com/referenceworkentry/10.1007/978-1-4939-0790-8_44`

P. Elbau, L. Mindrinos, and O. Scherzer (2017). “Inverse problems of combined photoacoustic and optical coherence tomography”. In: *Mathematical Methods in the Applied Sciences* 40.3, pp. 505–522. ISSN: 0170-4214. DOI: `10.1002/mma.3915`. URL: `http://onlinelibrary.wiley.com/doi/10.1002/mma.3915/epdf`

P. Elbau, L. Mindrinos, and O. Scherzer (2018). “The inverse scattering problem for orthotropic media in polarization-sensitive optical coherence tomography”. In: *GEM - International Journal on Geomathematics* 9.1, pp. 145–165. DOI: `10.1007/s13137-017-0102-y`. URL: `https://link.springer.com/content/pdf/10.1007%2Fs13137-017-0102-y.pdf`

Quantitative Reconstruction in OCT

Assume the object is located inside a bounded domain $\Omega \subset \mathbb{R}^3$ and is characterized by the refractive index

$$n : \mathbb{R} \times \mathbb{R}^3 \to \mathbb{R},\ (k, x) \mapsto n(k, x),$$

with $n = 1$ outside Ω and $k = 2\pi/\lambda$ denotes the wavenumber.

Given the measurement data obtained by an OCT system, we are interested in extracting the refractive index of the underlying object from this data.

This means we are interested in inverting the equation

$$F(n) = 2\,\Re\mathrm{e}\left\{E_S(k, x, n) \cdot \overline{E_R(k, x)}\right\} = C$$

where F represents the OCT forward model.

Modeling Tasks

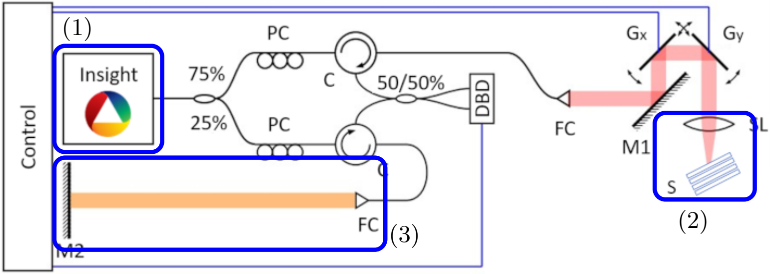

- (1) incident illumination
- (2) sample geometry and sample field
- (3) reference field

universität wien

Light as an Electromagnetic Wave

The light $E : \mathbb{R} \times \mathbb{R}^3 \to \mathbb{C}^3$ in presence of the object n and the illumination $E^{(0)} : \mathbb{R} \times \mathbb{R}^3 \to \mathbb{C}^3$ is modeled by an electromagnetic wave propagating through space.

Maxwell's Equations in Frequency Domain

$$\begin{aligned} \nabla \times \nabla \times E(k,x) - k^2 n^2(k,x) E(k,x) &= 0, && k \in \mathbb{R}, x \in \mathbb{R}^3, \\ E(k,x) &= E^{(0)}(k,x) + E_S(k,x), && k \in \mathbb{R}, x \in \mathbb{R}^3 \end{aligned}$$

The incident field is modeled as vacuum solution. Additionally, we require that $\operatorname{supp} \mathcal{F}_k^{-1}(E^{(0)})(ct,.) \cap \Omega = \emptyset$ for all $t < 0$.

$$\begin{aligned} \Delta E^{(0)}(k,x) + k^2 E^{(0)}(k,x) &= 0, && k \in \mathbb{R}, x \in \mathbb{R}^3, \\ \nabla \cdot E^{(0)}(k,x) &= 0, && k \in \mathbb{R}, x \in \mathbb{R}^3. \end{aligned}$$

universität wien

A Look at Experimental Data

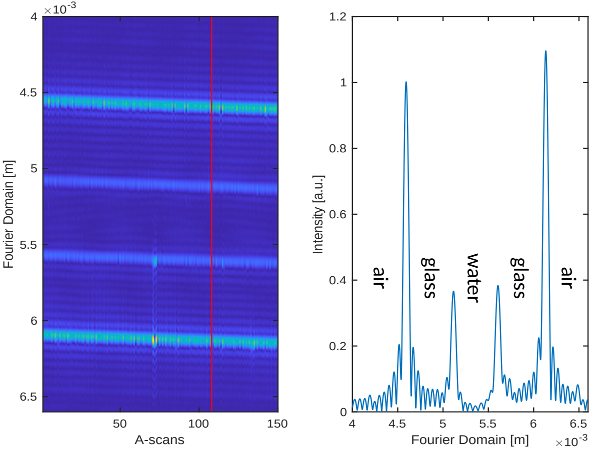

Figure: Fourier transformed OCT data of a three layer glass-water-glass sample. The refractive indices of the coverglass and water are known for all wavenumbers used in the OCT system. Courtesy by Lisa Krainz, Medical University of Vienna.

Redefined Geometry

- Within the illuminated region, the object shows layered structure, meaning that

$$\Omega = \bigcup_{j=1}^{J} \Omega_j, \quad n(k,x) \approx \delta(x_1)\delta(x_2)n(k,x_3) = \chi_{\Omega^c}(x_3) + \sum_{j=1}^{J} \chi_{\Omega_j}(x_3) n_j(k).$$

  Due to the small bandwidth of the OCT system, we assume $n_j(k) \equiv n_j \in \mathbb{R}$.

- Simplifies Maxwell's equation to Helmholtz problem.

- This form of geometry has been discussed multiple times:

O. Bruno and J. Chaubell (2005). "One-dimensional inverse scattering problem for optical coherence tomography". In: *Inverse Problems* 21, pp. 499–524. ISSN: 0266-5611

P. H. Tomlins and R. K. Wang (2005). "Theory, developments and applications of optical coherence tomography". In: *Journal of Physics D: Applied Physics* 38, pp. 2519–2535

P. Elbau, L. Mindrinos, and L. Veselka (2021). "Quantitative OCT reconstructions for dispersive media". In: *Time-dependent Problems in Imaging and Parameter Identification*. Ed. by B. Kaltenbacher, T. Schuster, and A. Wald. Green-OA. Springer, Cham, pp. 229–266. DOI: https://doi.org/10.1007/978-3-030-57784-1_8

Plane Wave Illumination

by **Adolf Fercher**:

"...the weakly inhomogeneous object is illuminated by the waist of an optical Gaussian beam. Hence, within a depth extension of the order of magnitude of the Rayleigh length we can assume plane-wave illumination..."

A. F. Fercher, W. Drexler, C. K. Hitzenberger, and T. Lasser (2003). “Optical coherence tomography - principles and applications”. In: *Reports on Progress in Physics* 66.2, pp. 239–303

Plane Wave Illumination

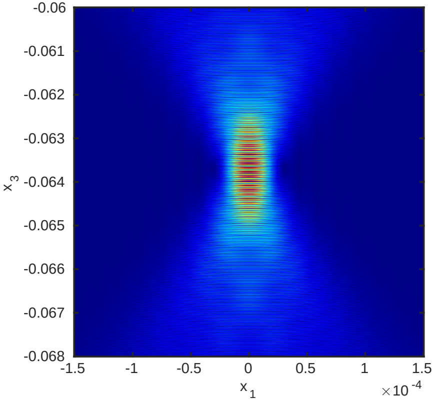

Figure: Incident laser light on a lateral-axial grid. The red line indicates the focus position, the red dashed line the Rayleigh length.

Plane Wave Illumination

by **Adolf Fercher**:
"...the weakly inhomogeneous object is illuminated by the waist of an optical Gaussian beam. Hence, within a depth extension of the order of magnitude of the Rayleigh length we can assume plane-wave illumination..."

Within the waist of a Gaussian beam, we may assume

$$E^{(0)}(k,x) = e^{-ikx_3}e_2, \quad e_2 = (0,1,0).$$

This allows us to analytically calculate the reflected field E_S up to a finite order of multiple reflections.

Plane Wave Illumination

by **Adolf Fercher**:
"...the weakly inhomogeneous object is illuminated by the waist of an optical Gaussian beam. Hence, within a depth extension of the order of magnitude of the Rayleigh length we can assume plane-wave illumination..."

Within the waist of a Gaussian beam, we may assume

$$E^{(0)}(k,x) = e^{-ikx_3} e_2, \quad e_2 = (0,1,0).$$

This allows us to analytically calculate the reflected field E_S up to a finite order of multiple reflections. The cross-correlation is given by

$$C(k) = \sum_{j=1}^{J} R_j \cos\left(2k\left(\Delta_0 + \sum_{l=1}^{j-1} n_l d_l\right)\right), \quad R_j \approx \frac{n_{j-1} - n_j}{n_{j-1} + n_j}, \; d_l = |\Omega_l|.$$

A. F. Fercher, W. Drexler, C. K. Hitzenberger, and T. Lasser (2003). “Optical coherence tomography - principles and applications”. In: *Reports on Progress in Physics* 66.2, pp. 239–303

universität wien

Basic Idea of Reconstruction

Best case possible: C is obtained for all wavenumbers $k \in \mathbb{R}$

$$C(k) = \sum_{j=1}^{J} R_j \cos\left(2k\left(\Delta_0 + \sum_{l=1}^{j-1} n_l d_l\right)\right)$$

$$\underset{\mathcal{F}_k^{-1}}{\overset{\mathcal{F}_k}{\longleftrightarrow}} \quad \mathcal{I}(z) = \sum_{j=1}^{J} R_j\, \delta\left(z - 2\left(\Delta_0 + \sum_{l=1}^{j-1} n_l d_l\right)\right)$$

O. Bruno and J. Chaubell (2005). "One-dimensional inverse scattering problem for optical coherence tomography". In: *Inverse Problems* 21, pp. 499–524. ISSN: 0266-5611

P. Elbau, L. Mindrinos, and L. Veselka (2021). "Quantitative OCT reconstructions for dispersive media". In: *Time-dependent Problems in Imaging and Parameter Identification*. Ed. by B. Kaltenbacher, T. Schuster, and A. Wald. Green-OA. Springer, Cham, pp. 229–266. DOI: https://doi.org/10.1007/978-3-030-57784-1_8

Basic Idea of Reconstruction

Fourier transformed simulated data for a three layer model: in blue the 'almost' best case for a large bandwidth, in red the actual bandwidth.

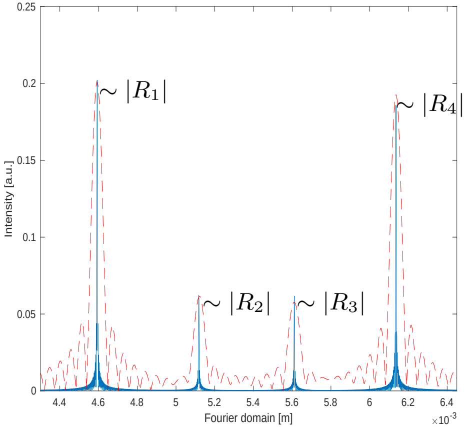

Basic Idea of Reconstruction

Basic Idea of Reconstruction

Fourier transformed simulated data for a three layer model: in blue the 'almost' best case for a large bandwidth, in red the actual bandwidth.

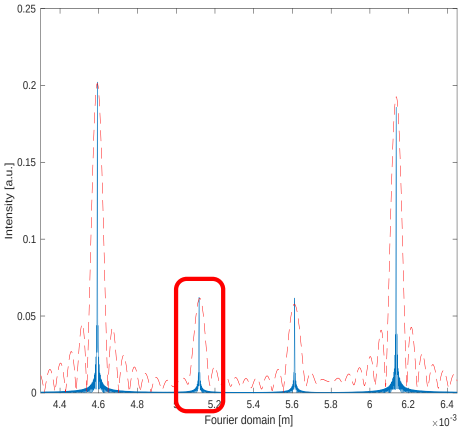

Basic Idea of Reconstruction

simulated data "reconstruction" (based on plane wave model)

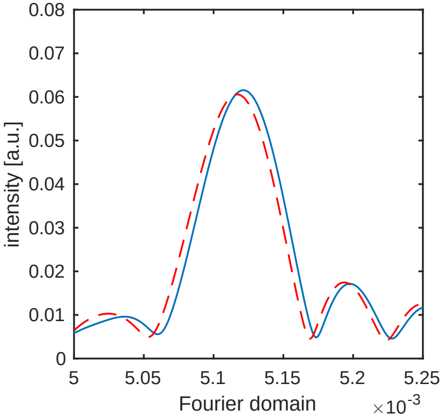

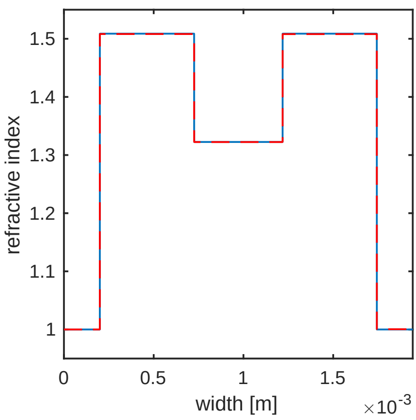

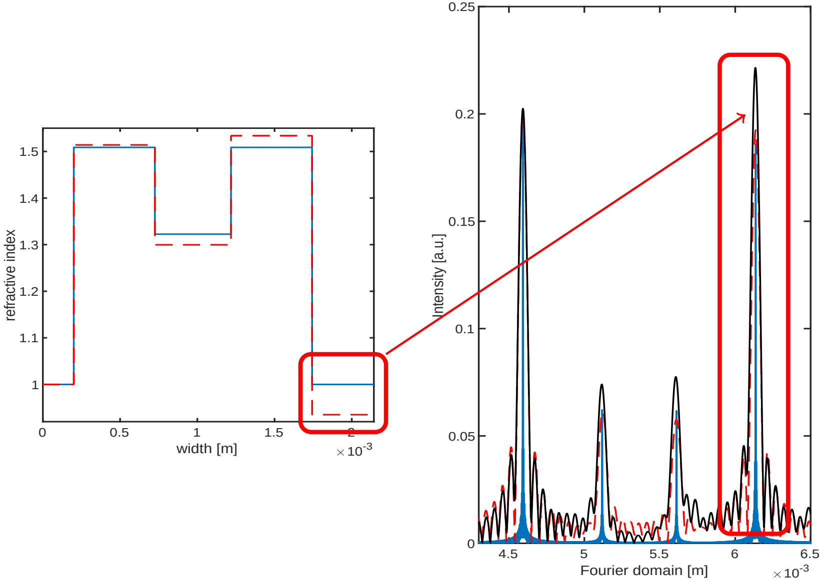

refractive index
1.5
1.4
1.3
1.2
1.1
1
0
0.5
1
1.5
2
width [m]
$\times 10^{-3}$
Intensity [a.u.]
0.25
0.2
0.15
0.1
0.05
0
4.5
5
5.5
6
6.5
Fourier domain [m]
$\times 10^{-3}$

The mismatch between the plane wave model and the experimental data originates from in a regular behaviour. $\longrightarrow$ **Focusing effects?**

The mismatch between the plane wave model and the experimental data originates from in a regular behaviour. $\longrightarrow$ **Focusing effects?**

Tested the idea:

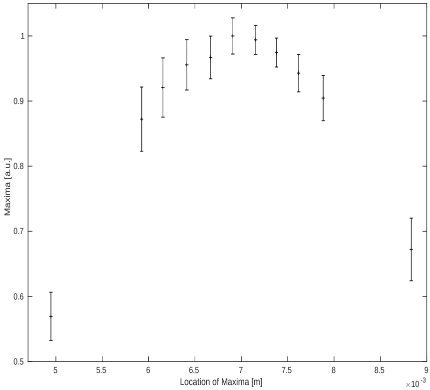

Figure: The mean intensities $\tilde{\mathcal{I}}_m$ (with errorbars) for different positions with respect to the focus.

The object (a perfectly reflecting mirror) is shifted along the axial direction and at every step an OCT measurement was performed. We consider the mean intensity over a Bscan, that is for $m = 1, \ldots, M$

$$\tilde{\mathcal{I}}_m = \frac{1}{L} \sum_{l=1}^{L} \max_z |\mathcal{I}_l(z)| \, .$$

Plane wave model $\longrightarrow \tilde{\mathcal{I}}_m \equiv \tilde{\mathcal{I}}$ for all m.

universität
wien

Gaussian Beam Model

Let $r_0 \in \mathbb{R}$, we specify data in the focus

$$E^{(0)}(x_1, x_2, r_0) = f(x_1, x_2)\eta, \quad (x_1, x_2) \in \mathbb{R}^2,\ \eta \in \mathbb{S}^1 \times \{0\}$$

Here, $f : \mathbb{R}^2 \to \mathbb{R}$ is such that $\mathcal{F}_{x_{12}}(f)$ has support in $D_{|k|}(0)$.

Restrict to the downward propagating field (in direction of $-x_3$), which takes

$$E^{(0)}(x) = \frac{1}{8\pi^2} \int_{D_{|k|}(0)} \mathcal{F}_{x_{12}}(f)(\kappa)\tilde{\eta}(\kappa) e^{i\kappa\cdot x_{12}} e^{-i\sqrt{k^2-|\kappa|^2}(x_3-r_0)} d\kappa.$$

typically: $\mathcal{F}_{x_{12}}(f)(\kappa) = e^{-|\kappa|^2 a},\ a > 0.$

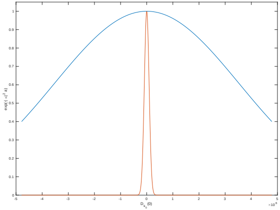

T. S. Ralston, D. L. Marks, P. S. Carney, and S. A. Boppart (2006). "Inverse scattering for optical coherence tomography". In: *Journal of the Optical Society of America A* 23.5, pp. 1027–1037. ISSN: 0764-583X

L. Veselka, L. Krainz, L. Mindrinos, W. Drexler, and P. Elbau (2021). "A Quantitative Model for Optical Coherence Tomography". In: *Sensors* 21.20. Hybrid-OA, p. 6864. DOI: 10.3390/s21206864. URL: https://www.mdpi.com/1424-8220/21/20/6864

Reflected Field for Gaussian Incident

The assumption of an object showing layered structure

$$n(x_3) = \chi_{\Omega^c}(x_3) + \sum_{j=1}^{J} \chi_{\Omega_j}(x_3) n_j.$$

again allows, by decomposing the incident field into plane waves, a computation of the reflected field. For a single reflection that is

$$E_S(x) \simeq \int_{D_{|k|}(0)} \mathcal{F}_{x_{12}}(f)(\kappa) R(\kappa) e^{-i\Psi_0(\kappa)} e^{ik_r(\kappa)\cdot x} d\kappa$$

- $R(\kappa) \approx R = \frac{1-n_1}{1+n_1}$ reflection coefficient
- $k_r(\kappa)$ is the reflected vector
- Ψ_0 includes focus position, sample surface, layer distances

Observations:

1.) Coupling into the transport fiber, discards all waves with large deviation from the main propagation direction.

$$\mathcal{B} = \left\{ \kappa \in \mathbb{R}^2 \;\middle|\; k_r(\kappa) \cdot e_3 \geq k \cos\theta \right\}$$

θ is called the maximal angle of acceptance

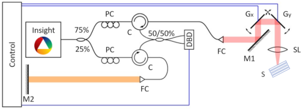

2.) Angular dependence (in far field):
for fixed $s \in \mathbb{S}^2_+$, as $\rho \to \infty$

$$E_S(\rho s) = E_{S,\infty}(\rho s) + o(1/\rho), \quad \left| E_{S,\infty}(\rho s; \theta_\Omega) \right|^2 \simeq \frac{1}{\rho^2} e^{-\left(k \sin(2\theta_\Omega)\sqrt{2a}\right)^2}$$

3.) Approximation by the far-field pattern only under conditions: let $r_0 < 0,\ \theta_\Omega = 0$, then for $\psi_0 = r_0 - 2x_{\Omega,3}$

$$E_S(0) = \frac{k}{ak - \frac{i}{2}\psi_0} \left(1 - e^{-k^2 \sin^2\theta a} e^{i\frac{k}{2}\psi_0 \sin^2\theta}\right) e^{-ik\psi_0}$$

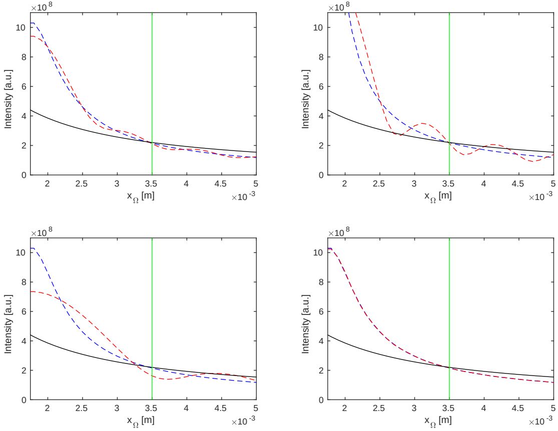

Figure: The far-field approximation (black), the Gaussian near field (red) and the Gaussian near field in for the "limit $\theta \to \infty$" (blue) for different sample positions $x_{\Omega,3}$. The green line denotes the focus position r_0. The near field in red is presented for different values of a and θ.

Additional parameters a, θ, r_0 make a calibration necessary. Use the angular dependence and the shift experiment.

Comparison between real data and simulations: for the angular behaviour (left) and the focusing effect (right).

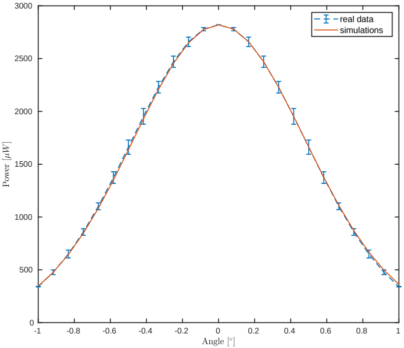

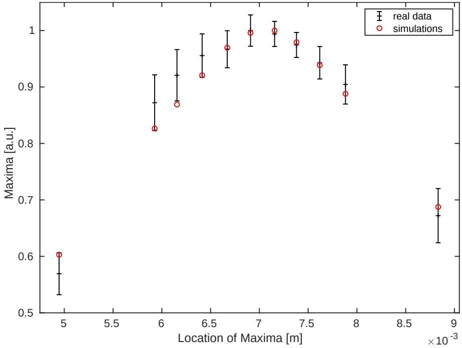

L. Veselka, L. Krainz, L. Mindrinos, W. Drexler, and P. Elbau (2021). "A Quantitative Model for Optical Coherence Tomography". In: *Sensors* 21.20. Hybrid-OA, p. 6864. DOI: 10.3390/s21206864. URL: https://www.mdpi.com/1424-8220/21/20/6864

Comparison with Data

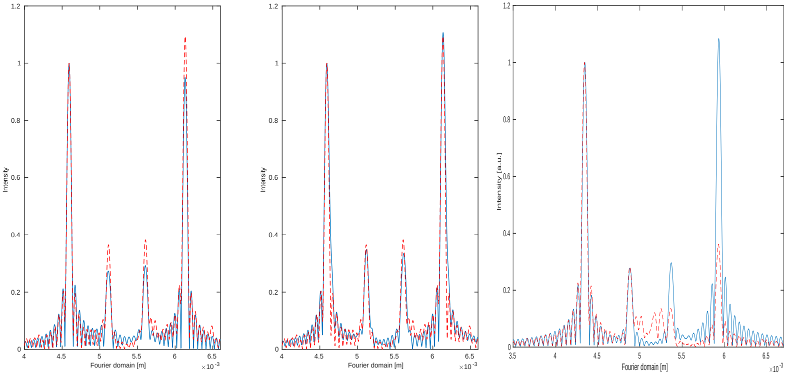

left: comparison of plane wave model and the presented Gaussian model, in blue, with the glass-water-glass sample in red

right: comparsion of the Gaussian model (blue) with milk data (red).

Summary & Conclusion

- For experimental data the Gaussian beam model seems advantageous compared to a single plane wave model.
- After the calibration of all necessary (system) parameters, the Gaussian model may be used for a reasonable reconstruction of all refractive indices.
- The calibration needs additional experiments.

Summary & Conclusion

- For experimental data the Gaussian beam model seems advantageous compared to a single plane wave model.
- After the calibration of all necessary (system) parameters, the Gaussian model may be used for a reasonable reconstruction of all refractive indices.
- The calibration needs additional experiments.

Thank you for your attention!